Proceedings of the 7th European VLBI Network Symposium
Bachiller, R. Colomer, F., Desmurs, J.F., de Vicente, P. (eds.)
October 12th-15th 2004, Toledo, Spain

Probing the polarization characteristics of SS433 on mas scales

Z. Paragi[1], R.C. Vermeulen[2], D.C. Homan[3], J.F.C. Wardle[4], I. Fejes[5], R.T. Schilizzi[6,7], R.E. Spencer[8], A.M. Stirling[8]

[1]JIVE, Postbus 2, 7990 AA Dwingeloo, The Netherlands,[2]ASTRON, Postbus 2, 7990 AA Dwingeloo, The Netherlands,[3]Denison Univ., Physics Dep., Granville, OH 43023, United States,[4]Brandeis Univ., Physics Dep., MS 057, P.O. Box 549110, Waltham, MA 02454-9110, United States,[5]FÖMI SGO, P.O. Box 585, H-1592 Budapest, Hungary,[6]International SKA project Office, 7990 AA Dwingeloo, The Netherlands,[7]Leiden Obs., P.O. Box 9513, 2300 RA Leiden, The Netherlands,[8]JBO, Jodrell Bank, Macclesfield, Cheshire, SK11 9DL, United Kingdom

Abstract.
We present a status report of dedicated circular polarization (CP) global VLBI observations of SS433. The total intensity image of the source is presented. We do not detect linear polarization in the core region of the source. We estimate the errors in D-terms for the EVN, and its effect on the final right-left circular polarization gain calibration. The data from this and earlier observations are analyzed with the "zero-V" self-calibration technique, in order to obtain indications for detectable CP in different regions of the source. Our data show no evidence for strong gyro-synchrotron (GS) emission on the size scale probed by our beam.

1. Introduction

SS433, is a microquasar (radio-jet X-ray binary system). It ejects antiparallel beams at a near relativistic velocity of 0.26c (see Vermeulen 1995 and references therein). High resolution EVN experiments showed that the radio core of the source has double core-wing morphology (Vermeulen et al. 1993). Recent observations with the VLBA and the EVN revealed that the compact jet region is similar in many respects to the radio cores observed in quasars. These observations also showed evidence for an "equatorial outflow" in the system, unprecedented in radio-jet sources before (Paragi et al. 1999a, 2002). The equatorial emission region was also imaged in an experiment using the phased VLA, MERLIN and the VLBA (Blundell et al. 2001).

The beams of SS433 are unique in the sense that they contain baryonic matter evidenced from Doppler-shifted spectral lines observed in the optical regime (e.g. Margon 1984 and references therein) and X-rays (e.g. Kotani et al. 1996). They also contain highly relativistic electrons (with Lorentz factors $\gamma \sim 300$) radiating by the synchrotron process. The low-energy cutoff of this electron population – just as in other microquasars or quasars – is not known. But the contribution of 1–100 MeV electrons ($\gamma = 2 - 200$) to the total luminosity may give rise to detectable amount of circular polarization (CP) in the source (Spencer & McCormick 2003).

Recently it was demonstrated – in spite of the difficulties with calibration – that circular polarization can be detected in quasars with the VLBI technique, using the VLBA array (Wardle et al. 1998). The CP emission is related to the radio core of the sources that is assumed to be a transition region where radiation becomes optically thin. In microquasars CP emission was detected in GRS1915+105 (Fender et al. 2002) and SS433 (Fender et al. 2000) with connected-element interferometers. There is no high resolution observation obtained to date that shows circular polarization in these sources.

2. The global VLBI observations

We carried out global VLBI observations of SS433 on 29 May 2003, including several calibrator sources dedicated for CP calibration. The array consisted of the western EVN, the VLBA, the Green Bank Telescope, and a single dish of the VLA. The observing frequency was 1.6 GHz. The recording rate was 256 Mbps using 2 bit sampling. There were two 16 MHz channels recorded in both RCP and LCP polarizations. This setup was used because we wanted to maximize the channel sensitivity, which simplifies the fringe-finding procedure a great deal, given the target source can be detected in data from a single channel. All channels were related to the lower sideband of the video converters. This, coupled with the fact that the experiment had a fan-out 1:4 caused complications in correlation. The correlator control software at JIVE had to be upgraded in order to handle this mode properly.

The data calibration was carried out in AIPS. In a first attempt, we used the amplitude calibration information provided by the EVN Pipeline (Reynolds, Garrett & Paragi 2002). However we realized that much of the T_{sys} data were missing for the Green Bank Telescope. To avoid unnecessary flagging of data due to missing calibration information, we inserted T_{sys} values in each scan, typical for the sources. In the case of Noto and Torun we found that the stokes V values were in excess of 10%. The problem with calibrating these stations is under investigation. These three stations could not be included in our CP analysis.

For correcting the polarization leakage D-terms and calibrating the gain of the R and L systems, we included five bright sources (~ 1 Jy) in the experiment: OQ208, 3C345, NRAO512, J1832+1357, J2002+4725. Circular polarization has not been detected in these sources to date. After parallactic angle correction we run task LPCAL in AIPS. This was done for all calibrators, to estimate how accurate our D-term calibration was (Table 1). Eventually we used the D-terms from OQ208, which is practically unpolarized.

After applying the D-terms we imaged all the calibrator sources in Difmap. The next step will be the proper calibration of the right and left handed system gains, using all the calibrator sources. The idea is that, on average, these have no circular polarization. Any source that has significant CP with respect to the others has to be left out from this procedure (Homan & Wardle 1999). This work is still under progress.

3. Polarization purity of the array and possible effects on the CP calibration

Determining circular polarization with VLBI is the art of calibrating the gains for the left and right handed systems properly (Homan & Wardle 1999). For the VLBA, the effect of polarization leakage is rather small. However for the EVN it is worth estimating how the D-terms might affect the CP calibration in an experiment.

The polarization-leakage D-terms of the telescopes are listed in Table 1. The statistical errors were estimated from solutions using different calibrator sources. These errors are in fact upper limits, because there is an uncertainty in the polarization structure of the calibrators as well. We used the solutions from OQ208, which is not affected by this error since it is unpolarized. The errors were in general below the 1% level in D-term amplitude for the array. Green Bank and Westerbork had slightly higher errors. These stations may have had a variable D-term throughout the experiment. The scatter in D-term phases was order of 10% for the EVN, and order of 20% for the US array. There are a couple of stations where very large phase errors are listed. In these cases one or two phase solutions had the wrong sign, while their absolute value was close to the other ones. It is not clear what causes this uncertainty of phase solutions in LPCAL.

The circular polarization (stokes V) is formed from the ideal RR and LL correlations as $V = (RR-LL)/2$. The measured quantities are described by the leakage term model (Cotton, 1993). For baseline mn, r^{RR}_{mn} and r^{LL}_{mn} can be written as:

$$r^{RR}_{mn} = g^R_m g^{R*}_n [e^{-j(\alpha_m-\alpha_n)} \cdot RR + D^R_m e^{j(\alpha_m+\alpha_n)} \cdot LR + D^{R*}_n e^{-j(\alpha_m+\alpha_n)} \cdot RL + D^R_m D^{R*}_n e^{j(\alpha_m-\alpha_n)} \cdot LL] \quad (1)$$

$$r^{LL}_{mn} = g^L_m g^{L*}_n [e^{j(\alpha_m-\alpha_n)} \cdot LL + D^L_m e^{-j(\alpha_m+\alpha_n)} \cdot RL + D^{L*}_n e^{j(\alpha_m+\alpha_n)} \cdot LR + D^L_m D^{L*}_n e^{-j(\alpha_m-\alpha_n)} \cdot RR], \quad (2)$$

where α_m is the parallactic angle at station m, g is the gain at the specified polarization, and * denotes complex conjugate. The measured stokes V becomes

$$r^V_{mn} = [e^{-j(\alpha_m-\alpha_n)}(g^R_m g^{R*}_n - g^L_m g^{L*}_n D^L_m D^{L*}_n) \cdot RR + e^{j(\alpha_m+\alpha_n)}(g^R_m g^{R*}_n D^R_m - g^L_m g^{L*}_n D^{L*}_n) \cdot LR + e^{-j(\alpha_m+\alpha_n)}(g^R_m g^{R*}_n D^{R*}_n - g^L_m g^{L*}_n D^L_m) \cdot RL + e^{j(\alpha_m-\alpha_n)}(g^R_m g^{R*}_n D^R_m D^{R*}_n - g^L_m g^{L*}_n) \cdot LL]/2. \quad (3)$$

Equations (1-3) show the complex way the D-terms are related to the station gains. For the simplest case of a non-polarized source ($RL = LR = 0$, $RR = LL = I$), the uncorrected D-terms would change the effective gain on a baseline in e.g. RR polarization in the following way: $G^R_{mn} = g^R_m g^{R*}_n (e^{-j(\alpha_m-\alpha_n)} + e^{j(\alpha_m-\alpha_n)} D^R_m D^{R*}_n)$. The errors in stokes V would be in the order of $D_m D_n$. In our case, the D-terms are calibrated to better than 1%, and so the effect of any D-term errors is at the level of $\sim 0.01\%$. Note that the errors may be larger for strongly polarized sources. In this case, we cannot neglect the $D \cdot RL$ and $D \cdot LR$ terms. Also note that a station with a variable D_m at the $\sim 1\%$ level introduces variations in the observed CP at the $1\% \times D_n$ level on baseline mn. In the case of the EVN, this means stokes V variations at levels of 0.1%, which is not negligible compared to the CP observed in the sources.

4. The core-region of SS433

The stokes I map of SS433 is shown on Fig. 1. We applied uniform weighting to the data to make the best possible use of the global array in terms of resolution. Overlaid on the map can be seen the precessional model of the source. We tried to find the kinematic centre for the moving jet components E_1 and W_1, assuming they were ejected at the same time, and varied the precession phase to get the best visual fit to the jet structure on the map. The observed precession phase was $\Psi = 0.72$ (using the model from Vermeulen 1989). At this precession phase the eastern jet is the approaching, and the western jet is the receding one. The kinematic centre, where the binary stellar system is located, was found to be off the brightest component. Earlier results showed (Paragi et al. 1999a) that the kinematic centre is located mid-way between the approaching and the receding core-jets. That region of the source is known to be heavily free-free absorbed by a spherically non-symmetric medium (Stirling, Spencer & Watson 1997; Paragi et al. 1999a). Our current result seems to be a bit different. At this epoch the brightness asymmetry between the approaching and the receding core-jet is larger than usual, and the E_{cw} feature seems to be closer to the kinematic centre than in previous observations.

There is emission surrounding the core region of the jets. It is more evident on the naturally weighted image (not shown). This feature is well known from previous observations (Blundell et al. 2001, Paragi et al. 1999a). One possible explanation is that this equatorial emission region is related to a non-relativistic outflow from the system (Paragi et al. 2002). The brighter equatorial features at $PA \sim 174$ and -25 degrees may indicate enhancements in the equatorial flow, which may have resulted in an increase in the free-free optical depth in the line of sight to the receding core-jet component.

We detect no linear polarization in SS433 on milliarcsecond scales. This result is consistent with earlier VLBI observations (Paragi et al. 1999b). The upper limit to the fractional polarization in the E_{cw} feature (estimated by dividing the 3 σ noise on the Q and U maps with the peak brightness in stokes I) is about 0.5%. The SS433 beams are known to be polarized on larger scales (e.g. Hjellming & Johnston 1981). Depolarization of the jets may occur in the same medium that is responsible for free-free absorption in the core. However the beams are depolarized up to scales of 100 mas, whereas free-free absorption occurs only in the innermost parts of the jet.

Table 1. Amplitudes (A_R, A_L) and phases (ϕ_R, ϕ_L) of the polarization leakage D-terms for the right and left systems, respectively. Amplitudes are given in percentages. The 1 σ errors were estimated from D-term values determined independently for each calibrator sources. For the US array, only the three brighter calibrators (3C345, OQ208, NRAO512) were used.

Code	$A_R \pm \sigma_R$	$\phi_R \pm \sigma_R$	$A_L \pm \sigma_L$	$\phi_L \pm \sigma_L$	Code	$A_R \pm \sigma_R$	$\phi_R \pm \sigma_R$	$A_L \pm \sigma_L$	$\phi_L \pm \sigma_L$
Ef	3.76±0.39	-80.33±8.06	7.53±0.67	-116.24± 6.55	SC	2.70±0.62	-51.65±199.86	1.51±0.25	-55.82± 3.00
Mc	11.00±0.62	7.20±3.11	17.95±0.68	105.08±156.55	HN	2.89±0.54	-44.43±12.17	1.45±0.48	142.82± 14.24
Wb	5.94±1.21	34.53±193.98	4.84±0.65	-112.91± 4.23	NL	2.77±0.67	64.38±191.72	2.34±0.69	49.87± 13.92
On	4.36±0.57	-49.17±7.83	3.72±0.50	-3.76± 2.83	FD	1.60±0.39	160.52± 23.53	3.33±0.11	-10.27± 8.68
Tr	7.76±0.37	117.31±5.49	6.87±0.38	69.32± 3.86	LA	1.73±0.98	-73.89±7.88	2.39±0.28	51.31±199.98
Nt	2.45±0.36	-47.32±7.88	3.07±0.22	59.41± 12.45	PT	3.70±0.16	-152.38±16.23	2.03±0.21	161.64± 14.30
Hh	5.57±1.15	139.52±14.84	7.44±0.43	42.84± 7.87	KP	2.98±0.60	-112.45±10.74	0.78±0.53	77.82± 16.34
Gb	3.19±0.71	-8.91±23.84	4.15±1.49	-151.17± 25.18	OV	1.72±0.98	139.58±20.44	0.94±0.66	52.49± 25.55
Y1	2.59±0.69	-52.45±12.81	2.51±0.51	-155.05± 12.07	BR	2.79±0.58	-150.93±22.04	3.69±0.73	56.54± 7.72
					MK	2.20±0.20	-63.11± 51.42	1.89±0.96	17.92± 16.40

5. Circular polarization in SS433

Circular polarization in SS433 was discovered by Fender et al. (2000) with the Australian Compact Array (ATCA). They observed a steep spectral index for the emission with $V \propto \nu^{-0.9\pm0.1}$. However, the fractional polarization could not be determined because the CP emission could not be resolved by ATCA. McCormick et al. (2003) monitored the source with ATCA for several months and found a long-term sign reversal in CP. The two main processes that may explain the observations is the synchrotron mechanism itself, and linear-to-circular polarization conversion (Kennett & Melrose 1998). Both of these processes require the presence of low-energy electrons. The predicted spectrum of the fractional circular polarization is $m_c \propto \nu^{-1/2}$ in the former case, while the spectral index maybe between -1 and -3 in the conversion models (see Fender et al. 2000 and references therein). Thus, if CP is detected on mas scales in SS433, multi-frequency high resolution observations may help us to find out which process is in action.

The location of the emitting region is also unclear at present. It can be the base of the jet as in quasars (Homan, Attridge & Wardle 1999), the larger scale radio beams, or the extended equatorial emission region. Spencer and McCormick (2003) suggested that the gyro-synchrotron (GS) process maybe effective as well if there is a significant fraction of electrons with Lorentz factor $\gamma \sim 30$. This could result in very high fractional circular polarizations. A good candidate region for this process to work is the equatorial emission for which thermal (Blundell et al. 2001) and synchrotron (Paragi et al. 1999a, 2002) origins have been proposed so far, none of which was fully confirmed.

An easy check for the GS scenario is self-calibrating the R and L systems with the total intensity model of the radio beams (i.e. assuming no circular polarization in the source). One may expect that some CP emission would show up at the location of the equatorial emission if the fractional CP was indeed high. We performed this test with our present data and global VLBI data taken in 1998, when the peak brightness of the equatorial region was the highest observed to date, around 8 mJy/beam. We see no indication of very high fractional CP from the equatorial emission, which means that we have no evidence for strong GS emission on the size scale probed by our beam.

6. Conclusions

Our observations showed that the receding core-jet of the system was fainter than usual. This may be due to a larger free-free optical depth in the equatorial outflow at the epoch of our observations. There is no linear polarization detected in SS433 on mas scales, with an upper limit to the fractional polarization of 0.5% in the core. The polarization leakage D-terms in our experiment were shown to be corrected to levels where they do not affect CP calibration significantly. Our early conclusion about the CP emission detected by others is that it is probably not due to the GS process. The nature of the equatorial emission remains unclear.

Acknowledgements. We would like to thank Chris Phillips to include our special observing mode in the correlator control software at JIVE. We are very grateful to Bob Campbell, who not only helped the PI during correlation, but also worked very hard on fixing the problems with the experiment. ZP acknowledges partial financial support from the Hungarian Scientific Research Fund (OTKA, grant No. T 046097). The National Radio Astronomy Observatory is operated by Associated Universities, Inc. under a Cooperative Agreement with the National Science Foundation. The European VLBI Network is a joint facility of European, Chinese, South African and other radio astronomy institutes funded by their national research councils. This research was supported by the European Commission's I3 Programme RadioNet, under contract No. 505818.

References

Blundell, K.M., Mioduszewski, A.J., Muxlow, T.W.B., Podsiadlowski, P., Rupen, M.P. 2001, Astrophys. J., 562, L79

Cotton, W.D. 1993, Astron. J., 106, 1241

Fender, R.P., Rayner, D., Norris, R., Sault, R.J., Pooley, G., 2000, Astrophys. J., 530, L29

Fender, R.P., Rayner, D., McCormick, D.G., Muxlow, T.W.B., Pooley G.G., Sault, R.J., Spencer, R.E., 2002, Mon. Not. R. Astron. Soc., 336, 39

Hjellming, R.M., Johnston, K.J., 1981, Nat., 290, 100

Homan, D.C., Wardle, J.F.C. 1999 Astron. J., 118, 1942

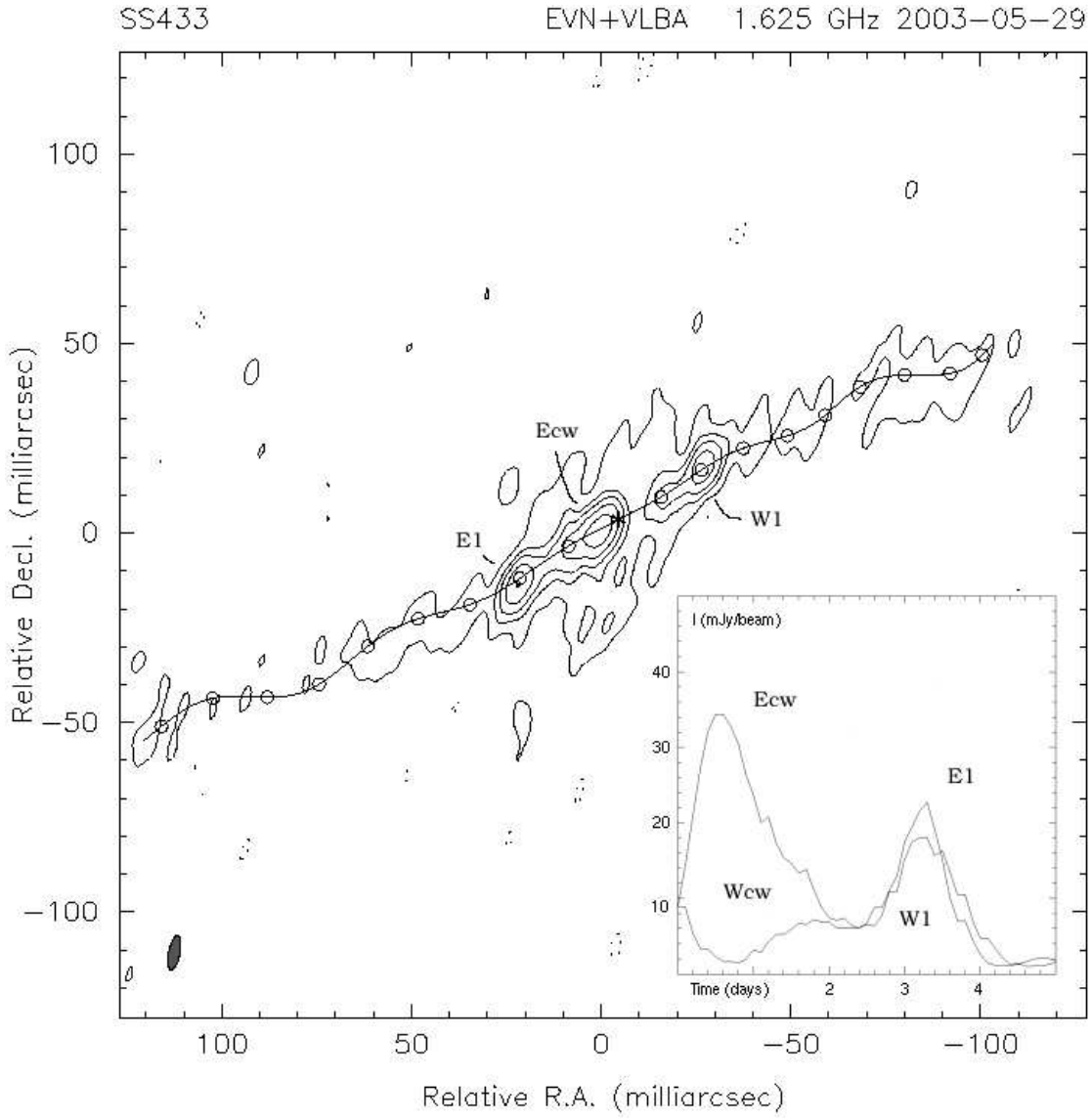

Fig. 1. Uniform weighted global VLBI map of SS433 on 29 May 2003, at 1.6 GHz. The contour levels are -2, 2, 4, 8, 16, 32, 64% of the peak brightness of 35.3 mJy/beam. The restoring beamsize is 9.19×2.98 mas, with the major axis oriented at PA=−11.3. Overlaid is the model of the precessing beams. The star indicates the kinematic centre, the open circles indicate the plasmon ejection time at every 1.6 days. The inset shows the brightness profiles of the approaching and the receding jets, with the ejection time – according to the precessional model – indicated.

Homan, D.C., Attridge, J.M., Wardle, J.F.C. 2001 Astrophys. J., 556, 113

Kennett, M., Melrose, D., 1998, Publ. Astron. Soc. Au., 15, 211

Kotani, T., Kawai, N., Matsuoka, M., Brinkmann, W., 1996, Publ. Astron. Soc. Japan, 48, 619

Margon, B., 1984, Ann. Rev. Astron. Astrophys., 22, 507

McCormick, D.G., Spencer, R.E., Fender, R.P., 2003, Astrophys. Space Sci., 288, 97

Paragi, Z., Vermeulen, R.C., Fejes, I., Schilizzi, R.T., Spencer, R.E., Stirling, A.M. 1999, Astron. Astrophys., 348, 910

Paragi, Z., Vermeulen, R.C., Fejes, I., Schilizzi, R.T., Spencer, R.E., Stirling, A.M. 1999, New Astron. Rev., 43,553

Paragi, Z., Fejes, I., Vermeulen, R.C., Schilizzi, R.T., Spencer, R.E., Stirling, A.M. 2002, Proc. 6th European VLBI Network Symposium, Ros. E., Porcas, R.W., Lobanov A.P., & Zensus J.A. (eds.), 2002, Bonn, Germany, pp. 263-266

Reynolds, C., Paragi, Z. & Garrett, M.A. 2002, Proc. XXVIIth General Assembly of the International Union of Radio Science', (Gent:URSI), session J8.P.4, paper No. 0924 (astro-ph/0205118)

Spencer, R.E., McCormick, D.G., 2003 Astrophys. Space Sci., 288, 193

Stirling, A.M., Spencer, R.E. & Watson, S.K., Vist. Astron., 41, 197

Vermeulen, R.C., 1989, Ph.D. thesis, Leiden University

Vermeulen, R.C., 1995, in: W. Kundt (ed.) Jets from Stars and Galactic Nuclei, p. 122, (Springer Verlag)

Vermeulen, R.C., Schilizzi, R.T., Spencer, R.E., Romney, J.D., I., Fejes, 1993, Astron. Astrophys., 270, 177

Wardle, J.F.C., Homan, D.C., Ojha, R., Roberts, D.H., 1998, Nat., 395, 457